

A novel hybrid carbon material

ALBERT G. NASIBULIN¹, PETER V. PIKHITSA², HUA JIANG³, DAVID P. BROWN¹,
ARKADY V. KRASHENINNIKOV^{4,5}, ANTON S. ANISIMOV¹, PAULA QUEIPO¹, ANNA MOISALA^{1*},
DAVID GONZALEZ¹, GÜNTHER LIENTSCHNIG⁶, ABDOU HASSANIEN⁶, SERGEY D. SHANDAKOV^{1†},
GIULIO LOLLI⁷, DANIEL E. RESASCO⁷, MANSOO CHOI², DAVID TOMÁNEK⁸ AND ESKO I. KAUPPINEN^{1,3‡}

¹NanoMaterials Group, Laboratory of Physics and Center for New Materials, Helsinki University of Technology, PO Box 1000, 02044, Espoo, Finland

²National CRI Center for Nano Particle Control, Institute of Advanced Machinery and Design, School of Mechanical and Aerospace Engineering, Seoul National University, Seoul 151-742, Korea

³VTT Biotechnology, PO Box 1000, 02044, Espoo, Finland

⁴Laboratory of Physics, Department of Engineering Physics and Mathematics, Helsinki University of Technology, 02044, Espoo, Finland

⁵Accelerator Laboratory, University of Helsinki, PO Box 43, FIN-00014, Helsinki, Finland

⁶Nanotechnology Research Institute, AIST, Tsukuba, Ibaraki 305-8568, Japan

⁷Chemical Biological and Materials Engineering, University of Oklahoma, 100 E Boyd SEC-T137, Norman, Oklahoma 73019, USA

⁸Physics and Astronomy Department, Michigan State University, East Lansing, Michigan 48824-2320, USA

*Present address: University of Cambridge, Department of Materials Science and Metallurgy, Cambridge, UK

†On leave from Kemerovo State University, Russia

‡e-mail: esko.kauppinen@hut.fi, albert.nasibulin@hut.fi

Published online: 25 February 2007; doi:10.1038/nnano.2007.37

Both fullerenes and single-walled carbon nanotubes (SWNTs) exhibit many advantageous properties¹. Despite the similarities between these two forms of carbon, there have been very few attempts to physically merge them^{2,3}. We have discovered a novel hybrid material that combines fullerenes and SWNTs into a single structure in which the fullerenes are covalently bonded to the outer surface of the SWNTs. These fullerene-functionalized SWNTs, which we have termed NanoBuds, were selectively synthesized in two different one-step continuous methods, during which fullerenes were formed on iron-catalyst particles together with SWNTs during CO disproportionation. The field-emission characteristics of NanoBuds suggest that they may possess advantageous properties compared with single-walled nanotubes or fullerenes alone, or in their non-bonded configurations.

NanoBuds have been synthesized in two different continuous aerosol (floating catalyst) reactors, by using particles grown *in situ* via ferrocene vapour decomposition⁴ and by using pre-made iron-catalyst particles produced by a hot wire generator⁵ (see Supplementary Information, Fig. S1). Transmission electron microscope (TEM) images of the product at low magnifications suggest that most synthesized SWNTs have an 'amorphous coating' (Fig. 1a). However, careful investigations (Fig. 1b–e) reveal that much of the coating in fact consists of fullerenes. Their spherical nature has been confirmed by tilting samples within a TEM. Statistical measurements of the spherical cages on the surface of SWNTs determined from high-resolution TEM images showed that the majority of the measured sizes can be attributed to the presence of C₄₂ and C₆₀ (Fig. 1f). Interestingly, the size distribution suggests the presence of C₂₀ fullerenes, the smallest possible dodecahedron. The key parameter required for NanoBud synthesis in both types of reactors was found to be the presence of trace concentrations of H₂O vapour and CO₂, thus

demonstrating the generality of the effect of these etching agents⁶ on catalytic fullerene/SWNT co-formation.

In an attempt to control the degree of SWNT coverage with fullerenes (that is, the degree of SWNT functionalization), we varied the reactor temperature and the concentrations of water vapour and carbon dioxide (see Supplementary Information, Fig. S2). We found that these parameters noticeably affect the amount of fullerenes on the surface of the SWNTs. The introduction of H₂O and CO₂ into the ferrocene reactor revealed that the optimum reagent concentrations were between 45 and 245 p.p.m. for water and between 2,000 and 6,000 p.p.m. for CO₂, and the highest fullerene density achieved was more than one fullerene per nanometre, with fullerenes arranged in a continuous stream along a SWNT.

It is known that non-covalently attached fullerenes are highly mobile on the surface of SWNTs under exposure to a TEM beam⁷, but our TEM observations showed NanoBud fullerenes to be stationary, indicating strong bonding. In order to further examine the nature of the fullerene–SWNT bond, we attempted both to evaporate and to dissolve the fullerenes from the surface of the SWNTs. Thermal treatment of the samples at 300–700 °C in inert helium or argon/hydrogen atmospheres showed no changes in the observed fullerene–SWNT structures (see Supplementary Information, Fig. S3). Careful washing of the NanoBuds in various solvents (hexane, toluene and decaline) also did not result in any significant alteration of the examined samples. Moreover, a mass-spectrometric investigation of the solvent after NanoBud washing did not reveal the presence of any dissolved fullerenes, further indicating a strong interaction between the fullerenes and SWNTs.

In order to elucidate the nature of the bond, spectroscopic and spectrometric methods, together with theoretical simulations, were applied. It is worth noting that Raman spectroscopy measurements

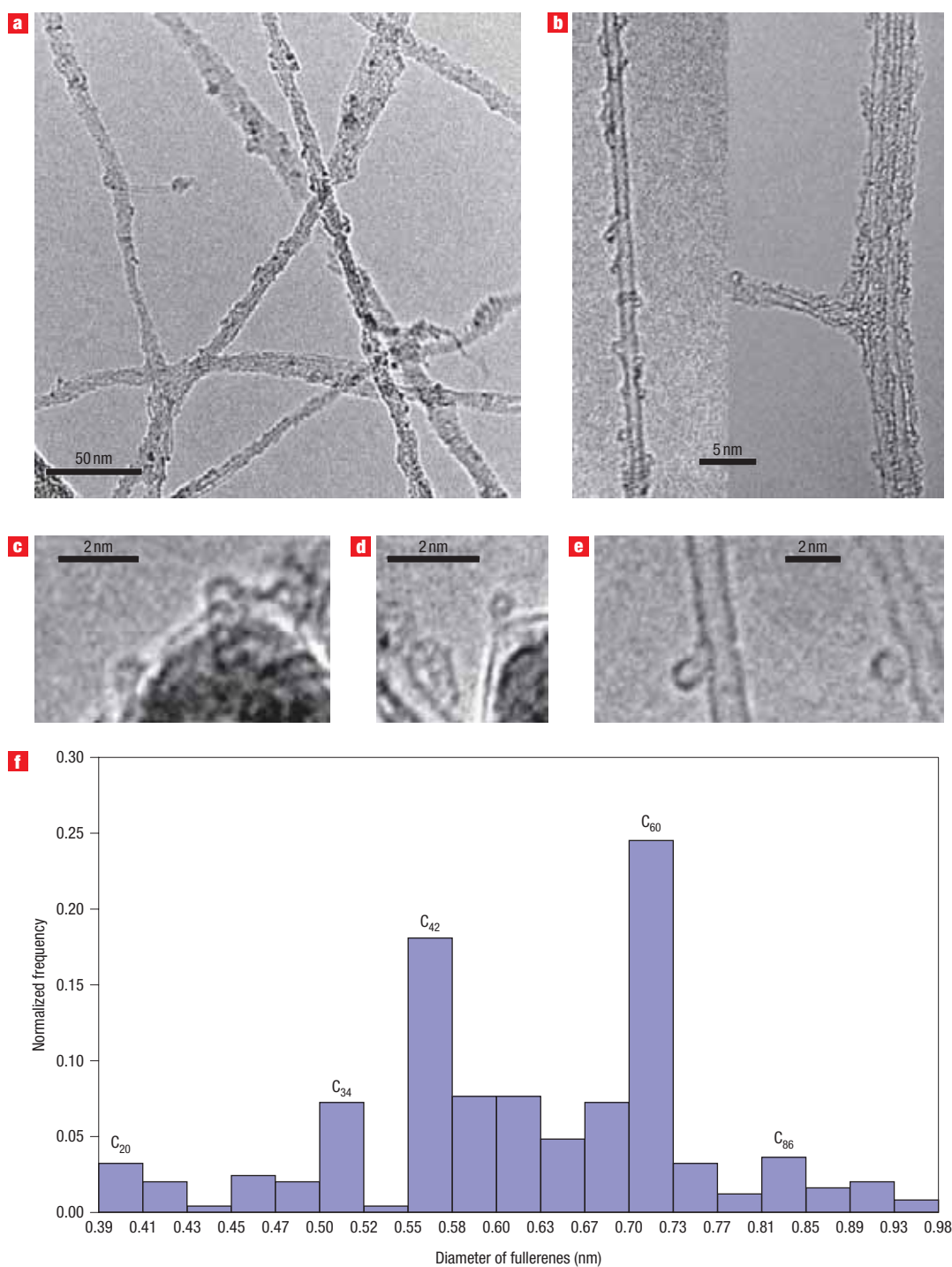


Figure 1 TEM observation of NanoBud structures. **a**, Low-magnification TEM image of a sample showing SWNTs seemingly covered by amorphous carbon. **b**, Intermediate-magnification TEM images of the sample, revealing the presence of spherical structures on the surface of the SWNTs. **c–e**, High-resolution TEM images showing fullerenes located on an iron-catalyst particle (**c**) and on a carbon layer covering a catalyst particle (**d**), and NanoBuds in which a fullerene is combined with a SWNT (left, **e**) and attached to the surface of a SWNT (right, **e**). **f**, Frequency–size distribution of fullerenes measured from high-resolution TEM images.

revealed only the presence of high-quality SWNTs, and did not detect the presence of fullerenes among the samples (see Supplementary Information), although they were visible in TEM images. Nevertheless, the ultraviolet–visible (UV–vis) absorption spectra of samples in *n*-hexane and toluene (Fig. 2a) are consistent with the TEM observation of the presence of both

SWNTs and fullerenes. Indeed, the characteristic ripple structure at wavelengths above 650 nm is known to be due to van Hove singularities of the SWNTs (refs 8 and 9). The higher-energy bands at 256, 279, 314, 330, 380 and 480 nm are close to those of the C_{70} fullerene (Fig. 2a), which is distinguished from spherical fullerenes (like C_{60}) by its ellipsoidal shape. Note that

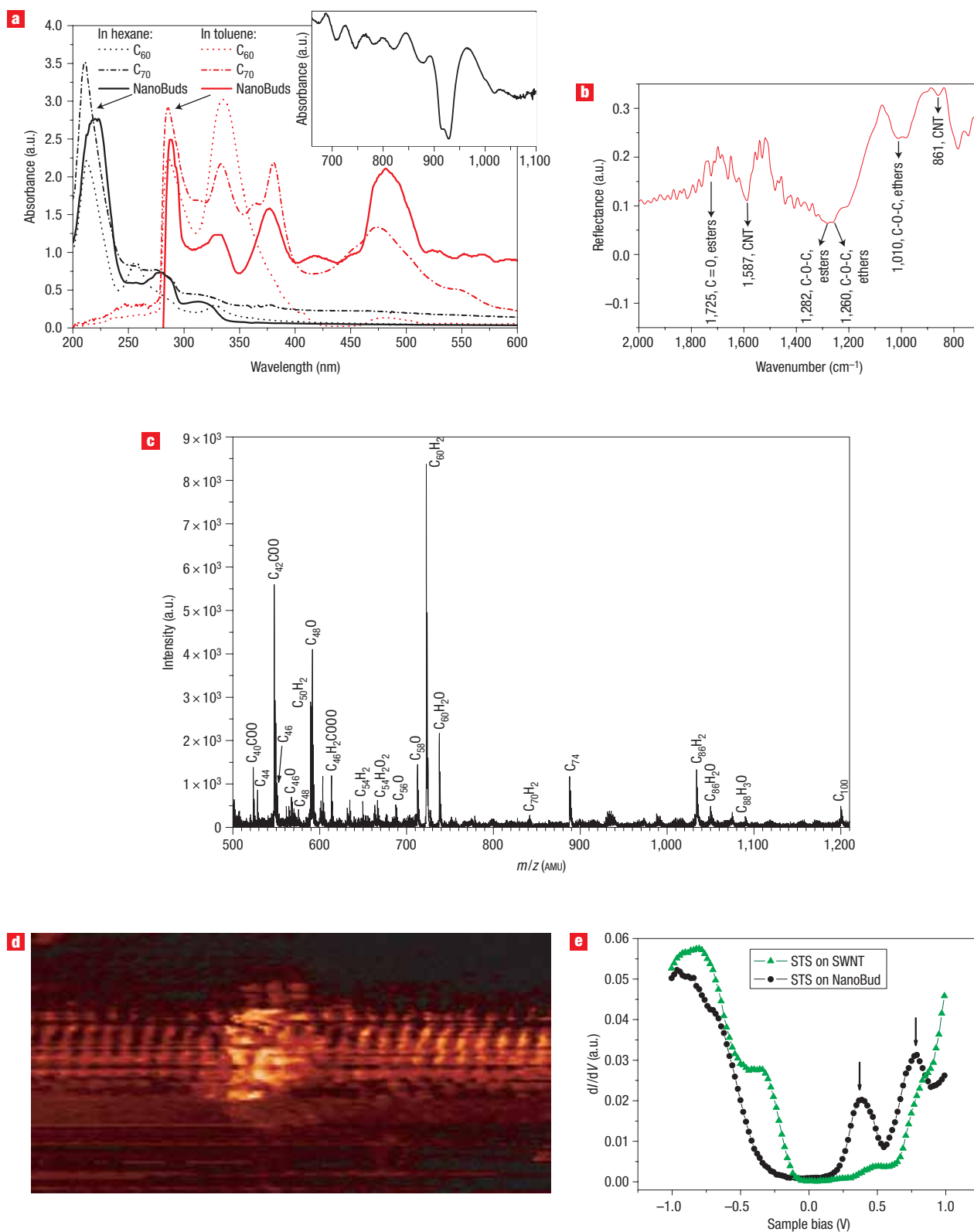


Figure 2 Characterization of NanoBuds. **a**, Comparison of UV-vis absorption spectra of NanoBuds with C_{60} and C_{70} standards in toluene (red lines) and hexane (black lines). NanoBud samples are shown as solid lines, and C_{60} and C_{70} standards are shown as dotted and dashed lines, respectively. Inset shows the low-energy absorption spectral ripple corresponding to van Hove singularities of SWNTs. **b**, Fourier transform infrared reflectance spectrum of NanoBuds showing the presence of ether (R-O-R) and ester (RO-O-R) groups in the sample. **c**, MALDI-TOF spectrum showing evidence for the presence of $C_{60}H_2$ and $C_{42}COO$, as well as other fullerenes containing O and H atoms. **d**, STM topographic image of a fullerene on the surface of a SWNT. The fullerene appears as a bright area on the SWNT. The size of the imaged area is 3.29×6.57 nm. **e**, STS measurements showing a comparison of the local density of states as a function of sample bias in the SWNT (green triangles) and NanoBud (black circles) structures.

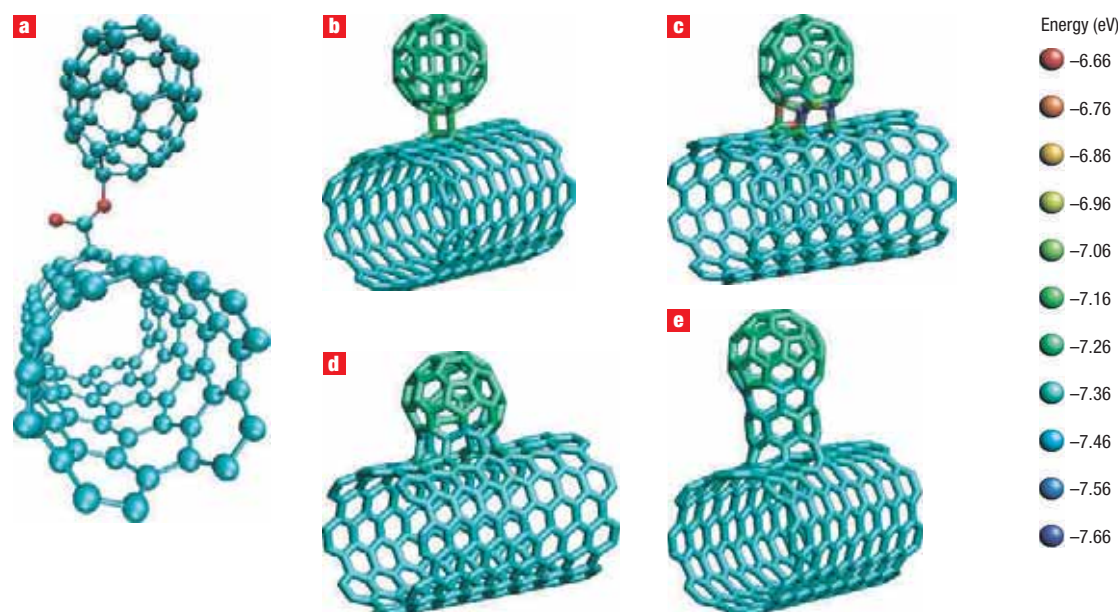


Figure 3 Bonding scenarios of fullerenes on SWNTs. **a**, C_{42} connected with a SWNT by an ester group. **b,c**, C_{60} chemisorbed on a defect-free (8,8) SWNT by [2+2] cycloaddition (**b**) and [4+4] cycloaddition (**c**). **d,e**, Fullerene–SWNT hybrid structures, reminiscent of buds on a branch. The relative binding energies of individual atoms in **b–e** are reflected by colour as shown on the right.

all ellipsoidal fullerenes such as C_{70} and C_{78} have similar UV spectra. Deviations from characteristic ‘bucky-ball’ peaks can be explained by the eccentric asymmetry induced by covalent/hybrid bonding of fullerenes to the SWNT. This asymmetry is thought to remove the degeneracy of the electron spectrum, thus revealing additional bands or broadening of existing peaks. In addition, the presence of covalently attached oxygen or hydrogen is known to restructure fullerene UV spectra^{10,11}. Electron energy loss spectroscopy measurements detected oxygen in all NanoBud samples (see Supplementary Information, Fig. S4).

Fourier transform infrared measurements were performed (Fig. 2b) to examine the possible role of oxygen in the NanoBuds. Characteristic peaks attributed to SWNTs (ref. 12) and both ether and ester groups¹³ are present in the spectrum. This was confirmed by matrix-assisted laser desorption ionization time-of-flight (MALDI-TOF) measurements. A spectrum obtained from a NanoBud sample in a T-2-(3-(4-*t*-butyl-phenyl)-2-methyl-2-propenylidene) malononitrile matrix prepared in dichloromethane solvent shows peaks of different ionized and hydrogenated fullerenes containing up to three oxygen atoms (Fig. 2c). The main spectrum peaks are attributable to C_{60} ($C_{60}H_2$, $C_{60}H_2O$) and C_{42} ($C_{42}COO$) fullerenes. MALDI-TOF results support the suggestion that at least some fullerenes are additionally connected to SWNTs by either ether (preferable for fullerenes larger than C_{54}) or ester (preferable for smaller fullerenes) bridges, although it is feasible that some of the observed oxygen can be present due to H_2O and CO_2 adsorbed on the fullerenes after synthesis.

In order to further investigate the structure of NanoBuds we have carried out scanning tunnelling microscopy (STM) and spectroscopy (STS) measurements of samples deposited on Au(111) substrates. Figure 2d,e shows a typical topographic image of a NanoBud and its electronic structure. The image displays an atomically resolved lattice in the vicinity of a fullerene, which is visible as a round protrusion above the

nanotube. Because of convolution effects, the observed size of the protrusion appears larger than it actually is. Unlike the physisorbed fullerenes, which can be easily manipulated by an STM tip¹⁴, the fullerene on the SWNT surface is robust and stationary against repetitive high-bias imaging, further confirming strong bonding to the SWNT. Figure 2e shows dI/dV as a function of bias voltage near and far away from the NanoBud. The most striking features for the NanoBud appear at positive sample biases, namely at 0.38 eV and 0.79 eV (indicated by the black arrows). These peaks cannot be assigned to a free or physisorbed fullerene. Another important feature is that the occupied states (see Fig. 2e under negative STM voltage) are also different from pure SWNT states and the peapod structure, in which unbound fullerenes are inserted inside SWNTs (refs 2 and 3). In peapods, only unoccupied states changed under positive voltage and the fullerene was ‘invisible’ under negative bias¹⁴. This fact clearly indicates the covalent nature of the fullerene–SWNT bond.

Our atomistic density-functional-theory based calculations¹⁵ have shown that systems composed of fullerenes covalently bonded through ester groups¹⁶ with single-vacancy SWNTs can indeed exist, although the assumed configurations are metastable with respect to forming perfect tubes together with oxidized fullerenes (Fig. 3a). Calculations with a model hamiltonian that has been successfully applied to describe the formation of peapods and the melting of fullerenes^{17,18} showed that fullerenes can be directly covalently bonded to SWNTs or can make hybrid structures. Results for the different adsorption scenarios of fullerenes on an (8,8) SWNT are summarized in Fig. 3b–e. We found that the structure formed through the chemisorption of perfect C_{60} molecules on SWNTs (Fig. 3b) via [2+2] cycloaddition is quite stable, but the configuration becomes unstable or marginally stable with respect to a defective SWNT and an isolated fullerene (Fig. 3c) in the case of [4+4] cycloaddition. One of the viable hybrid geometries involves imperfect fullerenes, covalently bonded to defective SWNTs. Such

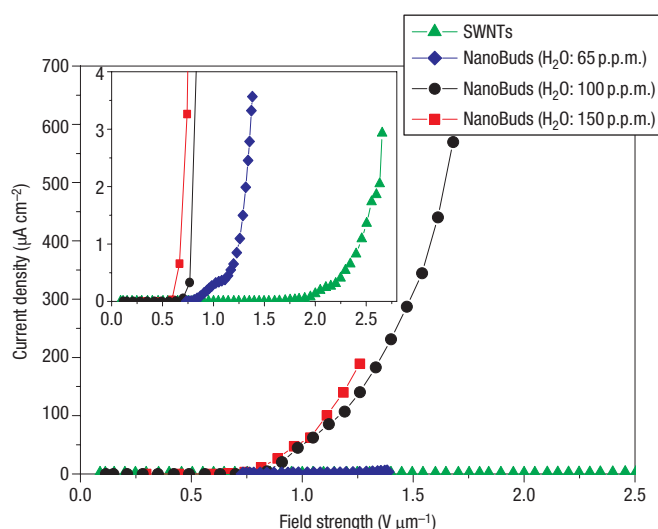


Figure 4 Field-emission properties of NanoBuds. Comparison of averaged current density against the electric field strength of NanoBuds (synthesized in a ferrocene reactor in the presence of 65, 100 and 150 p.p.m. of added water vapour) with a sample of SWNTs (synthesized without water vapour added). Inset shows close-up in the vicinity of the threshold voltage. Coverage of SWNTs by fullerenes increases with water vapour concentration (see Supplementary Information, Fig. S2), resulting in higher emission current.

bonded structures, reminiscent of buds on a branch, with a neck connecting the fullerene and the SWNT, are depicted in Fig. 3d,e, and can be recognized in high-resolution TEM images (Fig. 1e). The local binding energies in these structures (represented in colour) suggest that none of the carbon atoms is less stable than those in a C_{60} molecule.

In order to better understand the STM experimental results, we calculated the density of states (DOS), which can be associated with STM I–V curves, for the studied atomic structures (see Supplementary Information). It was found that the STS measurement (Fig. 2e) matches well with the DOS calculations carried out for the structure shown in Fig. 3b, where a fullerene C_{60} is attached to a SWNT by covalent bonds (cycloaddition). It is evident that covalent bonding between the fullerenes and nanotubes gave rise to new states between the first van Hove singularities, as was measured in the NanoBud samples. These states cannot be interpreted in terms of isolated (non-bonded) fullerenes because they do not coincide with the positions of peaks in the DOS of fullerenes alone. Thus, these calculations further support the suggestion that fullerenes and SWNTs are covalently bonded, as manifested by new states near the Fermi energy.

As for the mechanism of the hybrid material formation, TEM observations (Fig. 1c) suggest that both fullerenes and SWNTs originate from graphitic carbon precipitated on the surface of Fe nanoparticles catalysing CO disproportionation^{6,19,20}. This is supported by molecular dynamics simulation results^{21,22} predicting that various carbon nanostructures are formed on the surface of such catalysts. Recently, we have described a possible mechanism for SWNT formation at steady-state conditions, in which carbon continually precipitates on the catalyst particle surface to form an uninterrupted layer, partially covering the catalyst particle^{19,20}. Similarly, budding fullerenes can be formed on the surface of catalyst particles during the SWNT growth and transported to the growing tube wall as if on a conveyor belt. The

uniqueness of this method to produce fullerenes is supported by the fact that, although synthesis of fullerenes smaller than approximately C_{60} is typically not favoured in the presence of abundant hydrogen²³, we still readily observe small NanoBud fullerenes in samples produced in a hydrogen-rich environment.

NanoBuds are expected to be of interest for cold electron field emission due to the large number of highly curved fullerene surfaces acting as emission sites on conductive SWNTs. A comparison of field emission from unaligned in-plane deposited mats (with thicknesses from 0.5 to 1 μm) of NanoBuds and equivalent mats of SWNTs synthesized under similar conditions but without adding water vapour shows that NanoBuds exhibit a low field threshold of about $0.65 \text{ V } \mu\text{m}^{-1}$ and a much higher current density compared with pure SWNTs (Fig. 4). Note that the non-functionalized SWNTs have a field threshold for field emission as high as $2 \text{ V } \mu\text{m}^{-1}$. The electron emission properties of NanoBuds may make them attractive from an application point of view, as they are produced in a one-step continuous ambient pressure process and can be easily deposited directly after the reactor onto any substrate, including temperature-sensitive ones. In order to verify the stability of NanoBuds for potential applications in real devices, we performed multiple voltage scans at different field strengths for 90 min for each current (see Supplementary Information). The long-duration measurements, as well as post-experimental observation of the samples, revealed no significant degradation of the NanoBud samples, thus supporting the covalent nature of the bonding between SWNTs and fullerenes.

It can be expected that this novel material possesses other advantageous properties. For instance, because of the higher reactivity of fullerenes when compared with SWNTs, this hybrid material may open new avenues for functionalization through chemical modification. Additionally, the attached fullerene molecules would weaken bundling adhesion forces and thus would allow better dispersion of the material²⁴, and could be used as molecular anchors to prevent slipping of SWNTs in composites, thus improving the composite's mechanical properties. Moreover, owing to the charge transport between SWNTs and functionalizing fullerenes, both electrical and optical properties of the material can be tuned. The ability to directly synthesize SWNTs having distinct regions with different electronic properties is of importance for many applications, including memory devices, decoders and tuneable quantum dots²⁵.

In summary, we have synthesized a novel nanoscale carbon hybrid material, NanoBuds, consisting of fullerenes covalently attached to SWNTs. The evidence of their combined structures has been provided on the basis of TEM observations, spectroscopic and spectrometric investigations together with theoretical simulations. Our synthesis method is continuous, does not require multiple processing steps, and allows direct, ambient temperature deposition on any substrate, thereby eliminating the need for supporting substrates to tolerate NanoBud growth temperatures. Unaligned thin mats of in-plane deposited NanoBuds show promising field-emission properties.

Received 14 December 2006; accepted 18 January 2007; published 25 February 2007.

References

- Dresselhaus, M. S., Dresselhaus, G. & Eklund, P. C. *Science of Fullerenes and Carbon Nanotubes* (Academic Press, San Diego, 1996).
- Smith, B. W., Monthieux, M. & Luzzi, D. E. Encapsulated C_{60} in carbon nanotubes, *Nature* **396**, 323–324 (1998).
- Urita, K. Y. *et al.* Defect-induced atomic migration in carbon nanopeapod: tracking the single-atom dynamic behaviour. *Nano Lett.* **4**, 2451–2454 (2004).

- Moisala, A., Nasibulin, A. G., Shandakov, S. D., Jiang, H. & Kauppinen, E. I. On-line detection of single-walled carbon nanotube formation during aerosol synthesis method. *Carbon* **43**, 2066–2074 (2005).
- Nasibulin, A. G., Moisala, A., Brown, D. P., Jiang, H. & Kauppinen, E. I. A novel aerosol method for single walled carbon nanotube synthesis. *Chem. Phys. Lett.* **402**, 227–232 (2005).
- Nasibulin, A. G. *et al.* An essential role of CO₂ and H₂O during SWNT synthesis from carbon monoxide. *Chem. Phys. Lett.* **417**, 179–184 (2006).
- Smith, B. W. & Luzzi, D. E. Formation mechanism of fullerene peapods and coaxial tubes: a path to large scale synthesis. *Chem. Phys. Lett.* **321**, 169–174 (2000).
- Bachilo, S. M. *et al.* Structure-assigned optical spectra of single-walled carbon nanotubes. *Science* **298**, 2361–2366 (2002).
- O'Connell, M. J. *et al.* Band gap fluorescence from individual single-walled carbon nanotubes. *Science* **297**, 593–596 (2002).
- Weisman, R. B., Heymann, D. & Bachilo, S. M. Synthesis and characterization of the 'missing' oxide of C₆₀: [5,6]-open C₆₀O. *J. Am. Chem. Soc.* **123**, 9720–9721 (2001).
- Benedetto, A. F., Bachilo, S. M., Weisman, R. B., Nossal, J. R. & Billups, W. E. Photophysical studies of 1,2-C₇₀H₂. *J. Phys. Chem. A* **103**, 10842–10845 (1999).
- Eklund, P. C., Holden, J. M. & Jishi, R. A. Vibrational modes of carbon nanotubes; spectroscopy and theory. *Carbon* **33**, 959–972 (1995).
- Lin-Vien, D., Colthup, N. B., Fateley, W. G. & Grasselli, J. G. *The Handbook of Infrared and Raman Characteristic Frequencies of Organic Molecules* (Academic Press, Boston, San Diego, New York, London, Sydney, Tokyo, Toronto, 1991).
- Hornbaker, D. J. *et al.* Mapping the one-dimensional electronic states of nanotube peapod structures. *Science* **295**, 828–831 (2002).
- Frauenheim, T. *et al.* Atomistic simulations of complex materials: ground state and excited state properties. *J. Phys. Condens. Matter* **14**, 3015–3047 (2002).
- Banerjee, S., Hemraj-Benny, T. & Wong, S. S. Covalent surface chemistry of single-walled carbon nanotubes. *Adv. Mater.* **17**, 17–29 (2005).
- Berber, S., Kwon, Y.-K. & Tománek, D. Microscopic formation mechanism of nanotube peapods. *Phys. Rev. Lett.* **88**, 185502 (2002).
- Kim, S. & Tománek, D. Melting the fullerenes: a molecular dynamics study. *Phys. Rev. Lett.* **72**, 2418–2421 (1994).
- Nasibulin, A. G., Pikhitsa, P. V., Jiang, H. & Kauppinen, E. I. Correlation between catalyst particle and single-walled carbon nanotube diameters. *Carbon* **43**, 2251–2257 (2005).
- Nasibulin, A. G. *et al.* Studies on mechanism of single-walled carbon nanotube formation. *J. Nanosci. Nanotechnol.* **6**, 1233–1246 (2006).
- Shibuta, Y. & Maruyama, S. Molecular dynamics simulation of generation process of SWNTs. *Physica B* **323**, 187–189 (2002).
- Ding, F., Rosén, A. & Bolton, K. The role of the catalytic particle temperature gradient for SWNT growth from small particles. *Chem. Phys. Lett.* **393**, 309–313 (2004).
- Talyzin, A.V. *et al.* Gentle fragmentation of C₆₀ by strong hydrogenation: a route for synthesising new materials. *Chem. Phys. Lett.* **400**, 112–116 (2004).
- Graff, R. A. *et al.* Achieving individual-nanotube dispersion at high loading in single-walled carbon nanotube composites. *Adv. Mater.* **17**, 980–984 (2005).
- Yang, C., Zhong, Z. & Lieber, C. M. Encoding electronic properties by synthesis of axial modulation-doped silicon nanowires. *Science* **310**, 1304–1307 (2005).

Acknowledgements

We would like to thank V. Pore, A.-S. Jääskeläinen, M. Leskelä and Sangsun Yang for their assistance with UV-vis and field emission measurements. Financial support from the Academy of Finland and the Creative Research Initiatives Program supported by the Korean Ministry of Science and Technology is acknowledged. Partial financial support for this work has been provided by NSF NSEC grant no. 425826. G.L. thanks JSPS for financial support.

Correspondence and requests for materials should be addressed to E.I.K.

Supplementary information accompanies this paper on www.nature.com/naturenanotechnology

Author contributions

A.G.N., P.V.P. and E.I.K. conceived and designed the experiments. H.J., P.V.P., A.S.A., D.P.B., P.Q., D.G., A.M. and G.L. performed the experiments. A.G.N., P.V.P., E.I.K., D.B.P., S.D.S., D.E.R. and M.C. analysed and interpreted the data. A.G.N., D.P.B., P.V.P., E.I.K., A.H., A.V.K. and D.T. co-wrote the paper. A.V.K. is responsible for computer atomic simulations. G.L. and A.H. are responsible for STM measurements. All authors discussed the results and commented on the manuscript.

Competing financial interests

The authors declare that they have no competing financial interests.

Reprints and permission information is available online at <http://npg.nature.com/reprintsandpermissions/>